

Bent Lattice Models

Neelima Borade, Lingxin Cheng, and Eli Fonseca

August 7, 2020

1 Introduction

Exactly solvable lattice models have found numerous applications to the theory of symmetric functions among other areas of mathematics (See [1–7]). The terms solvable refers to the existence of a solution to the Yang-Baxter equation which often allows for explicit evaluation of the partition function [8, 9]. Knowing that a symmetric function is expressible as a partition function leads to a range of interesting combinatorial properties, including branching rules, Pieri and Cauchy-type identities.

In [10] Borodin and Wheeler introduced the notion of a colored lattice model. The process of adding color to a lattice model should be thought of as a refinement of the previously uncolored model. If one chooses the Boltzmann weights for the colored models appropriately, then one obtains a refinement of the (uncolored) partition function as a sum of partition functions indexed by all permutations of colors. Moreover, if the resulting colored model is solvable, then similar applications to those described above will follow. This idea was applied by Brubaker et al. [11] to study Type A Demazure atoms. Shortly after Brubaker et al. [12] showed how a colored refinement of the six-vertex model gives rise to a recursive method for computing all values of a basis of certain Whittaker functions again in Type A.

The goal of this report is to apply these ideas and go beyond the type A case. Explicitly we seek to evaluate the partition function for the bent lattice model of type \mathfrak{B} which was previously studied in [13] by using colored lattice models. To do this we use the U-turn square ice configurations from a paper of Hamel and King [14] of type \mathfrak{B} . In doing so we hope to recover the Demazure character for type \mathfrak{B} , whereas the partition function in [14] writes the partition function in terms of the universal character for the orthogonal group. This bent lattice model is displayed in 1.

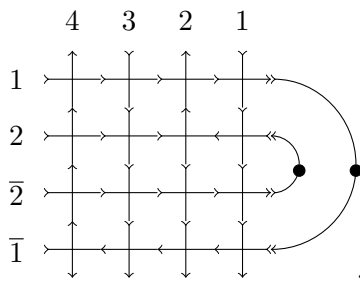


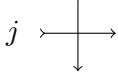
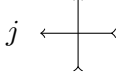
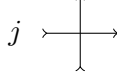
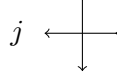
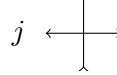
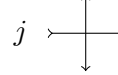
Figure 1: Admissible state of $\mathfrak{B}^{[4,2]}$

2 Boltzmann wieghts and Rectangular YBE

We want to translate the U-turn model in [14] to the bent model in [13] that we are interested in. To obtain the bent lattice model for the \mathfrak{B}^λ family in [13] we flip the corresponding U-turn

model in [14] about the vertical axis so that the bend appears on the right side, and about the horizontal axis so that the partition λ appears on the bottom boundary. This results in the bent model from [13], but the labelling of the rows is $\bar{1}, \bar{2}, \bar{n}, \dots, n, \dots, 1$ on the left boundary from top to bottom. This labelling of the rows is different from the one used in the [13], but we will compensate for this different labelling by adjusting our computations accordingly.

The figure below illustrates weights used by [14] for the U-turn model of type \mathfrak{B} . We will explain how to modify these to be used as weights for the bent model of type \mathfrak{B} from Figure 1.

					
$a_1^{(j)} = NW$	$a_2^{(j)} = SE$	$b_1^{(j)} = SW$	$b_2^{(j)} = NE$	$c_1^{(j)} = NS$	$c_2^{(j)} = EW$
$-y_j$	1	x_j	1	$x_j - y_j$	1

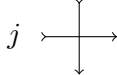
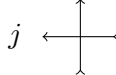
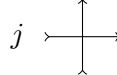
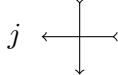
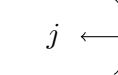
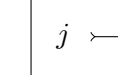
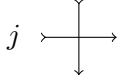
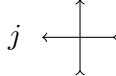
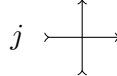
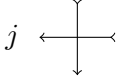
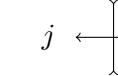
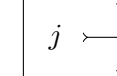
					
$a_1^{(j)} = NW$	$a_2^{(j)} = SE$	$b_1^{(j)} = SW$	$b_2^{(j)} = NE$	$c_1^{(j)} = NS$	$c_2^{(j)} = EW$
$-\bar{x}_{2n+1-j}$	1	\bar{y}_{2n+1-j}	1	$\bar{y}_{2n+1-j} - \bar{x}_{2n+1-j}$	1

Figure 2: Hamel and King weights from table 10.5 of [14]

Now we tabulate the weights for our bent lattice model \mathfrak{B}^λ obtained from those in Figure 2 by swapping the weights of configurations that are symmetric to each other about the vertical and horizontal axis, that is we swap N, S and E, W . We also swap the weights of z_i and $z_{\bar{i}}$ for $z \in \{a, b, c\}$ to compensate for the swapping of the bar rows and non bar rows mentioned earlier. Note that $\bar{z} = z^{-1}$ and $z_{2n+1-i} = \bar{z}_i$.

					
$a_1^{(j)} = NW$	$a_2^{(j)} = SE$	$b_1^{(j)} = SW$	$b_2^{(j)} = NE$	$c_1^{(j)} = NS$	$c_2^{(j)} = EW$
1	$-\bar{x}_{2n+1-i}$	1	\bar{y}_{2n+1-i}	$\bar{y}_{2n+1-i} - \bar{x}_{2n+1-i}$	1

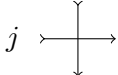
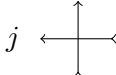
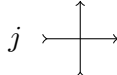
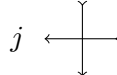
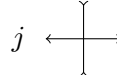
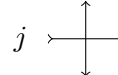
					
$a_1^{(j)} = NW$	$a_2^{(j)} = SE$	$b_1^{(j)} = SW$	$b_2^{(j)} = NE$	$c_1^{(j)} = NS$	$c_2^{(j)} = EW$
1	$-y_i$	1	x_i	$x_i - y_i$	1

Figure 3: Hamel and King weights applied to bent lattice model

We use Sage Math to compute a set of rotated vertices satisfying the rectangular YBE with

weights from Figure 3. The rectangular YBE is the following identity of partition functions :

$$\mathcal{Z} \left(\begin{array}{c} \phi \\ j \quad \alpha \\ k \quad \beta \\ \gamma \\ \epsilon \\ \delta \end{array} \right) = \mathcal{Z} \left(\begin{array}{c} \phi \\ j \quad \alpha \\ k \quad \beta \\ \gamma \\ \epsilon \\ \delta \end{array} \right)$$

for any choice of boundary arrow decorations $\alpha, \beta, \gamma, \delta, \epsilon, \phi$.

We know there is a set of rotated vertices satisfying the rectangular YBE by Proposition 1.1 of [14], since our weights are free-fermionic. Figure 4 lists these rotated vertices, where the rectangular YBE is applied to rows indexed by spectral parameters that do not have bars and Figure 5 lists the rotated vertices, where the rectangular YBE is applied to rows indexed by spectral parameters with bars.

$y_j - x_k$	$y_k - x_j$	$y_k - x_k$	$y_j - x_j$	$-y_k + y_j$	$x_j - x_k$

Figure 4: Rotated vertices for rows indexed by non-barred spectral parameters.

$-y_k + x_j$	$-y_j + x_k$	$-y_k + x_k$	$-y_j + x_j$	$x_j - x_k$	$y_j - y_k$

Figure 5: Rotated vertices for rows indexed by barred spectral parameters.

3 Checking bent YBEs

In the previous section we used found rotated vertices in Figure 4 and Figure 5 that satisfied the rectangular YBE for the modified weights in Figure 3. We want the weights from Figure 3 to give a simultaneous solution to the rectangular YBE and the bent ybes in Figure 8 of [13]. As our lattice model has bends on the right side, we require more local identities of partition functions, other than the rectangular YBE. Thus, we proceed to check the special types of YBEs from figure 8 of [13] using the weights from 4 and 5. We determine that these weights don't satisfy these YBEs along the bend.

Lemma 3.1. *The weights from Figure 4 and 5 don't satisfy the bent YBEs from [13].*

Proof. We examine each case and show the weights differ on both sides, that is before pushing a rotated vertex through a bend and after. Note that the bend vertices are assigned weight one as they do not appear in the model from Hamel and King's paper [14].

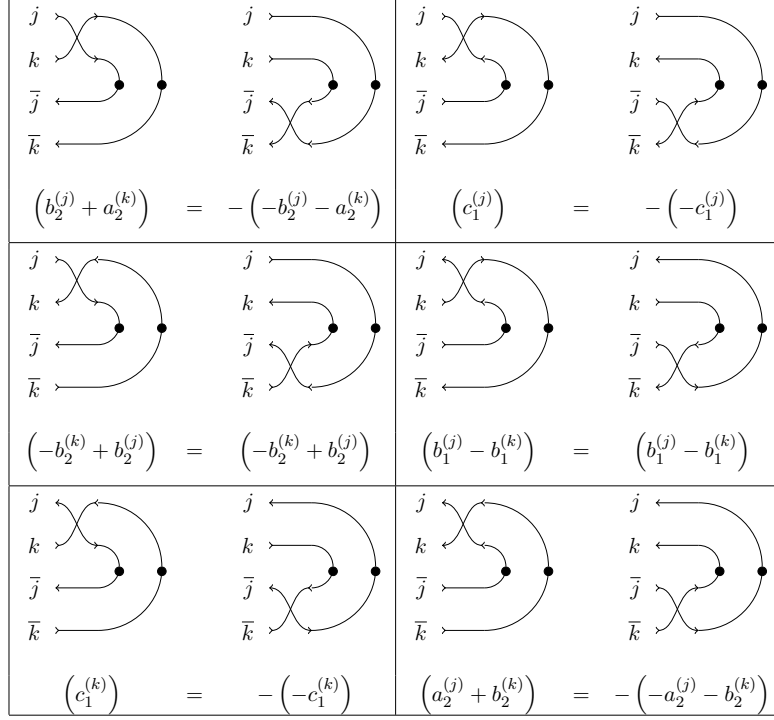


Figure 6: Bent YBE with Hamel and King weights

□

4 Modifying weights to satisfy bent YBEs.

We now perform a sign change by flipping the signs of some of the weights from Figure 3 such that the bent YBEs from Figure 6 hold. Specifically, we change the signs of a_2, b_2 and c_1 for the rows indexed by non-barred spectral parameters and the signs of a_1, b_2, c_1 for the rows indexed by barred spectral parameters. The weights are tabulated below.

$a_1^{(j)} = NW$	$a_2^{(j)} = SE$	$b_1^{(j)} = SW$	$b_2^{(j)} = NE$	$c_1^{(j)} = NS$	$c_2^{(j)} = EW$
1	\bar{x}_{2n+1-i}	1	$-\bar{y}_{2n+1-i}$	$-\bar{y}_{2n+1-i} + \bar{x}_{2n+1-i}$	1

$a_1^{(j)} = NW$	$a_2^{(j)} = SE$	$b_1^{(j)} = SW$	$b_2^{(j)} = NE$	$c_1^{(j)} = NS$	$c_2^{(j)} = EW$
-1	$-y_i$	1	$-x_i$	$-x_i + y_i$	1

Figure 7: Modified weights from Figure 2

We check which rotated vertices satisfy the rectangular YBE using [15] and obtain:

$y_j - x_k$	$y_k - x_j$	$y_k - x_k$	$y_j - x_j$	$-y_k + y_j$	$x_j - x_k$

Figure 8: Rotated vertices for both rows indexed by non-barred spectral parameters.

$y_k - x_j$	$y_j - x_k$	$y_k - x_k$	$y_j - x_j$	$x_j - x_k$	$y_j - y_k$

Figure 9: Rotated vertices for both rows indexed by barred spectral parameters.

We further show that the weights from Figure 3 after performing the sign change do satisfy the bent ybes from Section 4.

Lemma 4.1. *The weights from Figure 7 satisfy the bent YBEs from Figure 6.*

Proof. We verify this case by case as in the figure below.

$(-a_2^{(k)} - b_2^{(j)})$	$(-a_2^{(k)} - b_2^{(j)})$	$(b_2^{(k)} - b_1^{(j)})$	$(b_2^{(k)} - b_1^{(j)})$
$(b_2^{(k)} - b_1^{(j)})$	$(b_2^{(k)} - b_1^{(j)})$	$(a_2^{(j)} - a_2^{(k)})$	$(a_2^{(j)} - a_2^{(k)})$
$(-c_1^{(k)})$	$(-c_1^{(k)})$	$(-b_2^{(k)} - a_2^{(j)})$	$(-b_2^{(k)} - a_2^{(j)})$

Figure 10: Bent YBE with weights from Figure 8 and Figure 9

□

5 Acknowledgments

This research was carried out as part of the 2020 REU program at the School of Mathematics of the University of Minnesota, Twin Cities supported by NSF RTG grant DMS-1745638. The authors would like to thank Ben Brubaker, Claire Frechette, and Emily Tibor for their mentorship and support.

References

- [1] Fonseca, T. and Balogh, F.: The higher spin generalization of the 6-vertex model with domain wall boundary conditions and Macdonald polynomials. *Journal of Algebraic Combinatorics*. **41** (3), 843–866 (2014)
- [2] Borodin, A. and Wheeler, M.: Nonsymmetric Macdonald polynomials via integrable vertex models. 2019. arXiv: [1904.06804](https://arxiv.org/abs/1904.06804) [[math-ph](#)].
- [3] Wheeler, M. and Zinn-Justin, P.: Refined Cauchy/Littlewood identities and six-vertex model partition functions: III. Deformed bosons. *Advances in Mathematics*. **299**, 543–600 (2016)
- [4] Buciumas, V. and Scrimshaw, T.: Double Grothendieck polynomials and colored lattice models. 2020. arXiv: [2007.04533](https://arxiv.org/abs/2007.04533) [[math.CO](#)].
- [5] Bump, D., McNamara, P. J., and Nakasuji, M.: Factorial Schur functions and the Yang-Baxter equation. 2011. arXiv: [1108.3087](https://arxiv.org/abs/1108.3087) [[math.CO](#)].
- [6] Brubaker, B. et al.: Frozen Pipes: Lattice Models for Grothendieck Polynomials. 2020. arXiv: [2007.04310](https://arxiv.org/abs/2007.04310) [[math.CO](#)].
- [7] Brubaker, B., Bump, D., and Friedberg, S.: Schur Polynomials and The Yang-Baxter Equation. *Communications in Mathematical Physics*. **308**, 281–301 (2009)
- [8] Baxter, R.: The inversion relation method for some two-dimensional exactly solved models in lattice statistics. *J. Statist. Phys.* **28**, 1–41 (1982)
- [9] Baxter, R. J.: Exactly solved models in statistical mechanics. Academic Press Inc. [Harcourt Brace Jovanovich Publishers], London, 1982.
- [10] Borodin, A. and Wheeler, M.: Coloured stochastic vertex models and their spectral theory. 2018. arXiv: [1808.01866](https://arxiv.org/abs/1808.01866) [[math.PR](#)].
- [11] Brubaker, B. et al.: Colored five-vertex models and Demazure atoms. 2019. arXiv: [1902.01795](https://arxiv.org/abs/1902.01795) [[math.CO](#)].
- [12] Brubaker, B. et al.: Colored Vertex Models and Iwahori Whittaker Functions. 2019. arXiv: [1906.04140](https://arxiv.org/abs/1906.04140) [[math.RT](#)].
- [13] Brubaker, B. and Schultz, A.: The six-vertex model and deformations of the Weyl character formula. *Journal of Algebraic Combinatorics*. **42**, 917–958 (2014)
- [14] Hamel, A. and King, R.: Half-turn symmetric alternating sign matrices and Tokuyama type factorisation for orthogonal group characters. *Journal of Combinatorial Theory, Series A*. **131**, (2014)
- [15] The Sage Developers: SageMath, the Sage Mathematics Software System (Version 9.1). <https://www.sagemath.org>. 2020.